ACS Medicinal Chemistry Letters

Letter

pubs.acs.org/acsmedchemlett

Fluorescent Probes for Subcellular Localization during Osteclast Formation

Jing Wu, Qi Shen, Yue Wang, Dan Zhao, Chen Peng, and Jian-Xin Li*

State Key Lab of Analytical Chemistry for Life Science, School of Chemistry and Chemical Engineering, Nanjing University, Nanjing 210093, China

Supporting Information

ABSTRACT: Labeling of a small bioactive molecule with fluorescent probe has been becoming an essential tool in cell biology to reveal the subcellular distribution and the location of a molecular target. QOA-8a is a novel molecule with potent antiosteoporotic effect *in vivo*. To investigate the molecular mechanism of QOA-8a, novel fluorescence-tagged chemical probes as bioactive as their parent molecule were designed and synthesized. The fluorescent compound **12** showed a more potent inhibitory activity on RANKL-induced osteoclastogenesis at 2 μM compared with that of QOA-8a. Microscopy experiments revealed that almost all of probe **12** accumulated in the fusing region, with little in the osteoclast precursors or the mature osteoclasts during osteoclast formation. The result suggests the location of the binding target of QOA-8a, which might greatly narrow down the search field of the target protein(s).

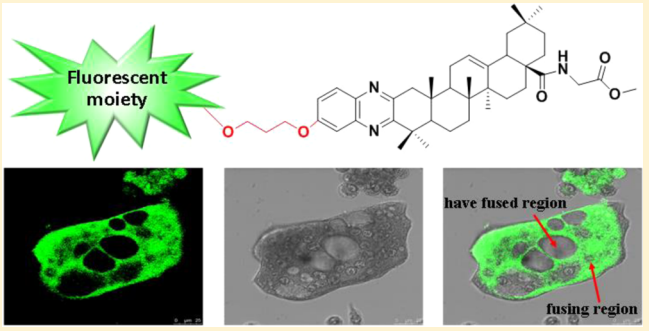

KEYWORDS: *Fluorescent derivative probes, osteoclasts, subcellular localization*

Fluorescent probe is a powerful tool offering a wealth of information on the subcellular localization, the location of a molecular target, and understandings of the biochemical events of a bioactive small molecule.[1] Designing of a fluorescent derivative as bioactive as its parent molecule can narrow down the search field and reduce compositional complexity of the sample (Figure 1).[2] For example, Kotake used ^{3}H-labeled, fluorescence-tagged, and photoaffinity-biotin-tagged "chemical probes" to successfully determine the subcellular localization and identify a 140 kDa protein in splicing factor SF3b as the binding target of an antitumor natural product, pladienolide.[3]

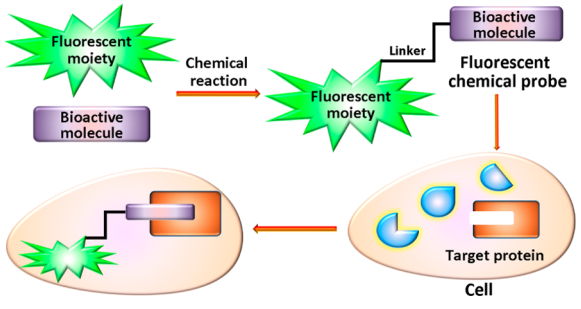

Figure 1. General concepts for designing of a fluorescent-tagged chemical probe.

Bone is a dynamic tissue capable of adapting its structure to mechanical stimuli and repairing structural damage through remodeling.[4] An imbalance in bone remodeling favoring resorption over formation underlies the pathology of many common and morbid skeletal diseases, such as osteoporosis.[4−8] Osteoclasts are large, multinucleated cells formed by the fusion of hematopoietic, mononuclear progenitors of the monocyte/macrophage lineage, and are responsible for resorbing bone. Medications targeting the osteoclasts, as the backbone of osteoporosis treatment can reverse this imbalance to improve bone quality and prevent fragility and pathologic fractures.[7−9]

In our previous reports, bioassay-guided isolation and structure elucidation revealed that the oleanolic acid and its glycosides possessed antiosteoporosis activity.[10,11] Further effort discovered that a quinoxaline derivative of oleanolic acid (QOA-8a) significantly inhibited the differentiation, formation, and bone resorptive activity of osteoclasts without cytotoxicity *in vitro*. In ovariectomized (OVX) mice, QOA-8a prevented the bone loss without any hormone-like side effects, and the OVX mice treated with 1 mg/kg/day of QOA-8a kept the same bone mineral density (BMD) as sham ones. The results suggested that QOA-8a might be a promising novel class of agent for the treatment of osteoporosis;[12,13] however, its mechanism is unclear.

In the present research, to make clear the subcellular localization of QOA-8a in osteoclasts and further investigate the molecular mechanism, novel fluorescent derivatives of QOA-8a were designed and synthesized. Considering the structural availability, fluorescent tags were designed to connect

Received: May 5, 2014
Accepted: June 11, 2014
Published: June 11, 2014

   dx.doi.org/10.1021/ml500181e | *ACS Med. Chem. Lett.* 2014, 5, 911−914

at two diverse positions of QOA-8a (Figure 2), and the inhibitory activity of the synthesized probes on receptor

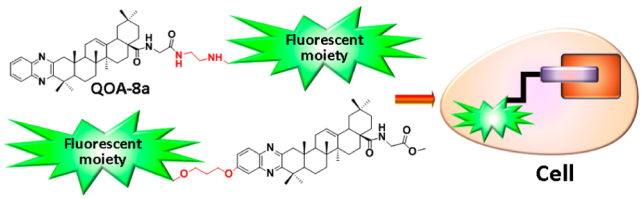

Figure 2. Design of fluorescent derivatives of QOA-8a.

activator for nuclear factor κB ligand (RANKL) induced osteoclast formation and their cytotoxicities were evaluated. Cellular localization of the probe with comparable bioactivity to parent compound was further imaged by confocal microscopy.

Dansyl and coumarin tags were commonly used in the fluorescent probe design.[14,15] First, we introduced those two tags at the amino acid moiety of QOA-8a to check their availability. Scheme 1 shows the outline for the synthesis of the

Scheme 1. Synthesis of Fluorescent Compounds 4 and 5[a]

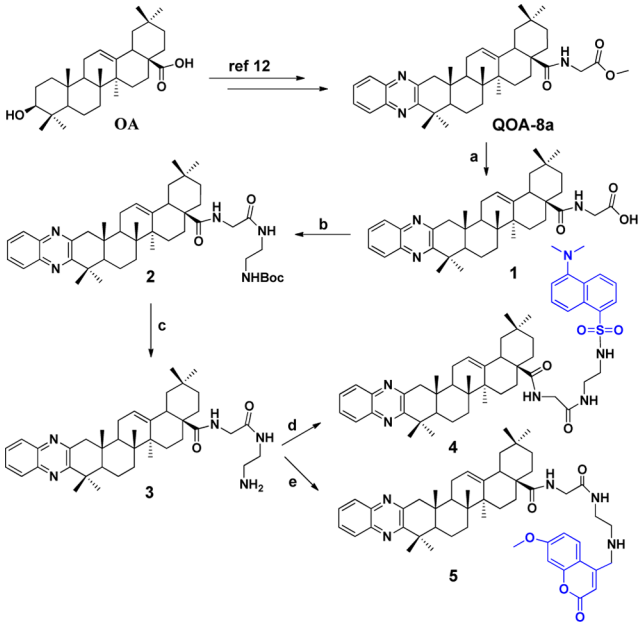

[a]Reagents and conditions: (a) NaOH, THF/H_2O, r.t., 4 h; (b) *tert*-butyl(2-aminoethyl)carbamate, HOBt, EDCI, TEA, DCM, r.t., overnight; (c) TFA, DCM, r.t., 0.5 h; (d) dansyl chloride, TEA, DCM, r.t., 2 h; (e) 4-bromomethyl-7-methoxycoumarin, K_2CO_3, acetone, 40 °C, overnight.

fluorescent compounds **4** and **5** from QOA-8a. During the first step, hydrolization of QOA-8a with NaOH in THF/H_2O afforded the desired acid **1** with a good yield. Coupling the acid with *tert*-butyl (2-aminoethyl) carbamate under HOBt/EDCI conditions gave compound **2**. Classical deprotection with TFA/DCM afforded key amine **3**. Reaction of this amine later alternatively with dansyl chloride in the presence of TEA in DCM or 4-bromomethyl-7-methoxycoumarin in the presence of K_2CO_3 in acetone afforded the fluorescent compounds **4** and **5**, respectively.

Next, guided by assay results (will be described later), we settled dansyl tag at quinoxaline moiety of QOA-8a. Preparations of fluorescent compounds **11**, **12**, **16**, and **17** are sketched in Scheme 2. Oxidation of OA using a Na_2WO_4–H_2O_2 system[16] gave key intermediate **6**, which was sequentially oxidized by *t*-BuOK/*t*-BuOH/O_2 to give intermediate **7**. Reaction of **7** with 3,4-diaminophenol afforded two isomers, **8** and **13**, without separation for the next step. Compounds **9** and **14** were prepared by stirring the mixtures of **8** and **13** with oxalyl chloride in anhydrous DCM, then treated with glycine methyl ester hydrochloride. In this step, isomers **9** and **14** could be easily separated by preparative TLC. Quinoxaline derivative **9** coupling with dansyl chloride in the presence of TEA yielded the desired fluorescent derivative **11**. Compound **9** underwent Williamson ether synthesis with 3-bromopropan-1-ol to yield corresponding compound **10**. Reaction of **10** with dansyl chloride gave the desired fluorescent derivative **12**. Fluorescent compounds **16** and **17** were obtained by the same protocol as described for preparation of compounds **11** and **12**.

Scheme 2. Synthesis of Fluorescent Compounds 11, 12, 16, and 17[a]

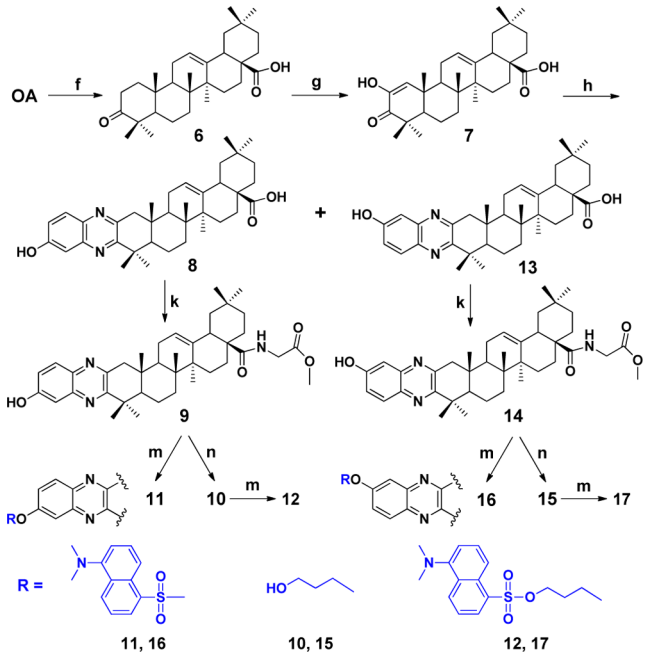

[a]Reagents and conditions: (f) Na_2WO_4/H_2O_2, $NaH_2PO_4{\cdot}2H_2O$/$Na_2HPO_4{\cdot}12H_2O$, DMF; (g) *t*-BuOK, *t*-BuOH, THF; (h) ethanol, **3**, 4-diaminophenol, 4 h; (k) (i) oxalyl chloride, DCM, r.t., 24 h; (ii) glycine methyl ester hydrochloride, Et_3N, DCM, 2 h; (m) dansyl chloride, TEA, DCM, r.t., overnight; (n) 3-bromopropan-1-ol, K_2CO_3, DMF, 60 °C, overnight.

It is unclear at which position (C-6′ or C-7′) the hydroxyl group of the isomers above is located. Attempts to use a single crystal to determine their stereostructures unfortunately failed. Therefore, detailed analyses of NOESY spectra were performed. As shown in Figure 3a, NOE correlation between signals H-8′ [δ 7.33 (d, J = 2.5 Hz, 1H)] and H_3-23 [δ 1.41 (s, 3H)] in **10** implied the hydroxyl group located at C-7′. In NOESY spectrum of **15**, a clear cross peak (Figure 3b) between H-8′ [δ 7.87 (d, J = 8.0 Hz, 1H)] and H_3-23 [δ 1.40 (s, 3H)] suggested that the hydroxyl group should be assigned at C-6′. Thus, the structures of **9**/**10** and **14**/**15** were elucidated as shown in Scheme 2.

dx.doi.org/10.1021/ml500181e | ACS Med. Chem. Lett. 2014, 5, 911–914

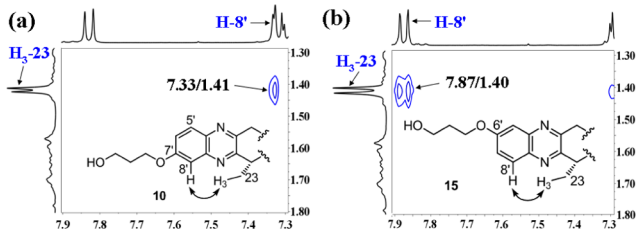

Figure 3. NOESY (solid arrow) correlations for compounds **10** (a) and **15** (b).

In our previous studies, QOA-8a inhibited RANKL-induced osteoclast formation generated from RAW264.7 cells at a nanomolar level.[12] To obtain fluorescence-tagged chemical probes as bioactive as their parent molecule, we screened fluorescent compounds using the same bioassay procedure as that of QOA-8a. The differentiation of mature osteoclasts was achieved using RAW264.7 cells with RANKL stimulation for 5 days *in vitro*. The mature osteoclasts are characterized as tartrate-resistant acid phosphatase ($TRAP^+$) multinucleated cells (red) containing three or more nuclei. First, the inhibitory activity of fluorescent compounds **4** and **5** was assayed to validate the reasonable tags. As shown in Table 1, both

Table 1. Inhibitory Activity of Synthesized Compounds against RANKL-Induced Osteoclast Differentiation on RAW264.7 Cells[a]

	inhibition (%) of OC[b]	
compd	10 μM	2 μM
4	100**	76.2 ± 6.2**
5	100**	60.6 ± 8.3**
9	100**	68.8 ± 10.8**
10	100**	52.6 ± 2.3**
14	100**	47.0 ± 9.7**
15	100**	87.8 ± 6.2**
11	72.7 ± 8.2**	65.2 ± 4.4**
16	98.2 ± 3.0**	67.8 ± 11.9**
12	100**	95.0 ± 0.6**
17	100**	74.9 ± 1.5**
QOA-8a	89.0 ± 3.5**	80.1 ± 1.3**

[a]See Experimental Section, Supporting Information. [b]Inhibition (%) = [(osteoclast number of control − osteoclast number of compound)/osteoclast number of control] × 100. Each data was expressed as mean ± S.D., $n = 3$. ** $p < 0.01$ vs control (0.0%).

compounds **4** and **5** possessed potent inhibitory activity on osteoclast formation at the concentration of 2 μM (76% inhibition of **4** and 60% of **5**), but a little bit weaker compared with that of the parent compound. With comparison of two fluorescent tags, dansyl-bearing compound **4** displayed a stronger inhibition compared to coumarin-bearing compound **5**. Thus, to obtain the most potent fluorescent probe, dansyl moiety was introduced to the quinoxaline moiety of QOA-8a.

As shown in Table 1, when dansyl moiety was directly connected to the hydroxyl group of the quinoxaline ring, compounds **11** and **16** remained strong, while weaker than QOA-8a. To prevent the loss of affinity and leave the inhibitory activity almost unchanged, the key isomers **10** and **15** with a β-propylene glycol linker were prepared, and a four-atom linker was introduced between the pharmacophore and the fluorescent tags. As a result, **10** and **15** displayed almost comparable inhibitory activity as the parent compound. Very meaningfully, when dansyl tag was introduced, the linker made **12** exhibit a stronger inhibitory activity on osteoclast formation (95.0%) compared with the parent compound at 2 μM. Figure 4 showed inhibitory effect of **12** on the formation of $TRAP^+$ multinucleated osteoclasts.

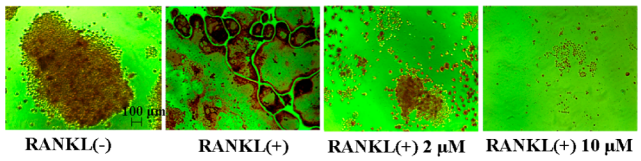

Figure 4. Inhibitory effect of probe **12** on RANKL-induced osteoclast formation.

To ascertain that the inhibitory activity of the fluorescent compounds on osteoclast formation was not due to their cytotoxicity, we assayed the cytotoxicity upon osteoclast precursor RAW264.7 cells by MTT method. The results revealed that these compounds showed no cytotoxicity up to the concentration of 10 μM (Table 2).

Table 2. Cytotoxicity of Compounds on Precursor of Osteoclasts (RAW264.7)[a]

compd	inhibition (%)	compd	inhibition (%)
control	0.0 ± 3.7	**12**	0.0 ± 6.4
4	0.0 ± 7.1	**14**	6.1 ± 6.1
5	0.0 ± 2.2	**15**	0.0 ± 1.1
9	0.0 ± 0.7	**16**	0.0 ± 1.9
10	0.0 ± 4.1	**17**	0.0 ± 4.3
11	0.0 ± 2.6		

[a]See Experimental Section, Supporting Information. The concentration of each compound was at 10 μM. No statistical differences vs control, $n = 3$.

Because of the potent inhibitory activity, compound **12** was chosen as the fluorescent probe for labeling osteoclasts. The dansyl moiety present in probe **12** allows a visible fluorescence at 515 nm when excited at 379 nm. The osteoclasts and their precursor RAW264.7 cells were incubated with **12** (5 μM) for 20 min, respectively. Observed by confocal microscopy, almost all of **12** accumulated in the fusing region (Figure 5C). Little was observed in the osteoclast precursors (Figure 5A) or the mature osteoclasts (Figure 5D). Cells at an early stage of differentiation or that have a fused region also had little fluorescent signal. The results suggested that the potent inhibitory activity of QOA-8a on osteoclast formation was mainly exerted during the highly fusing and differentiating period (Figure 5B).

In conclusion, novel fluorescent derivative probes for subcellular localization during osteoclast formation were synthesized. The most potent fluorescent probe **12** showed 95.0% inhibition at the concentration of 2 μM, which was as bioactive as its parent molecule. Confocal microscopy revealed a clear, subcellular localization of **12** that accumulated only in the highly fusing region. The results suggested the location of the binding protein of QOA-8a, which might greatly narrow down the search field. Our work may help in clarifying the molecular mechanism of antiosteoporosis activity of QOA-8a and pave the way of searching for its target protein(s).

dx.doi.org/10.1021/ml500181e | *ACS Med. Chem. Lett.* 2014, 5, 911−914

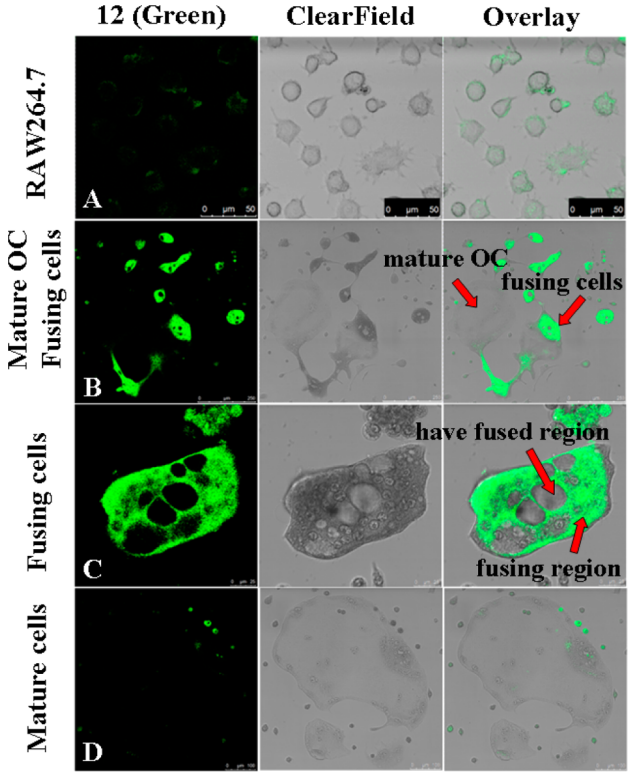

Figure 5. Cellular localization of fluorescent probe **12**. RAW264.7 cells and osteoclasts were, respectively, incubated with **12** (5 μM) for 20 min and imaged by confocal microscopy. Fluorescent probe **12** is presented as green.

■ ASSOCIATED CONTENT

Ⓢ Supporting Information

Synthetic experimental procedures, analytical data for compounds **1**−**17**, and details of biochemical assay methods. This material is available free of charge via the Internet at http://pubs.acs.org.

■ AUTHOR INFORMATION

Corresponding Author

*(J.-X.L.) Tel: +86-25-83686419. E-mail: lijxnju@nju.edu.cn.

Funding

We thank the National Natural Science Foundation of China (21272114 and 91313303) and the National Natural Science Fund for Creative Research Groups (21121091) for financial support.

Notes

The authors declare no competing financial interest.

■ ACKNOWLEDGMENTS

We thank Y. Shi and H. B. Mao for providing the MS assistance.

■ ABBREVIATIONS

OA, oleanolic acid; OC, osteoclast; RANKL, receptor activator for nuclear factor κB ligand; QOA-8a, quinoxaline derivative of oleanolic acid; TEA, triethylamine; TFA, trifluoroacetic acid; THF, tetrahydrofuran; DCM, dichloromethane; MTT, 3-(4,5-di-methylthiazol-2-yl)-2,5-diphenyltetrazolium bromide; HOBt, 1-hydroxybenzotriazole; EDCI, 1-(3-(dimethylamino)propyl)-3-ethyl-carbodiimide hydrochloride

■ REFERENCES

(1) Sato, S.; Murata, A.; Shirakawa, T.; Uesugi, M. Biochemical target isolation for novices: affinity-based strategies. *Chem. Biol.* **2010**, *17*, 616−623.

(2) Lenz, T.; Fischer, J. J.; Dreger, M. Probing small molecule−protein interactions: A new perspective for functional proteomics. *J. Proteomics* **2011**, *75*, 100−115.

(3) Kotake, Y.; Sagane, K.; Owa, T.; Mimori-Kiyosue, Y.; Shimizu, H.; Uesugi, M.; Ishihama, Y.; Iwata, M.; Mizui, Y. Splicing factor SF3b as a target of the antitumor natural product pladienolide. *Nat. Chem. Biol.* **2007**, *3*, 570−575.

(4) Robling, A. G.; Castillo, A. B.; Turner, C. H. Biomechanical and molecular regulation of bone remodeling. *Anun. Rev. Biomed. Eng.* **2006**, *8*, 455−498.

(5) Rossi, F.; Bellini, G.; Luongo, L.; Torella, M.; Mancusi, S.; Petrocellis, L. D.; Petrosino, S.; Siniscalco, D.; Orlando, P.; Scafuro, M.; Colacurci, N.; Perrotta, S.; Nobili, B.; Marzo, V. D.; Maione, S. The endovanilloid/endocannabinoid system: A new potential target for osteoporosis therapy. *Bone* **2011**, *48*, 997−1007.

(6) He, L.; Lee, J.; Jang, J. H.; Sakchaisri, K.; Hwang, J.; Cha-Molstad, H. J.; Kim, K.; Ryoo, I. J.; Lee, H. J.; Kim, S. O.; Soung, N. K.; Lee, K. S.; Kwon, Y. T.; Erikson, R. L.; Ahn, J. S.; Kim, B. Y. Osteoporosis regulation by salubrinal through eIF2α mediated differentiation of osteoclast and osteoblast. *Cell. Signalling* **2013**, *25*, 552−560.

(7) Miller, P. D. Denosumab: anti-RANKL antibody. *Curr. Osteoporosis Rep.* **2009**, *7*, 18−22.

(8) Kendler, D. L.; Roux, C.; Benhamou, C. L.; Brown, J. P.; Lillestol, M.; Siddhanti, S. Effects of denosumab on bone mineral density and bone turnover in postmenopausal women transitioning from alendronate therapy. *J. Bone Miner. Res.* **2010**, *25*, 72−81.

(9) Charles, J. F.; Coury, F.; Sulyanto, R.; Sitara, D.; Wu, J.; Brady, N.; Tsang, K.; Sigrist, K.; Tollefsen, D. M.; He, L.; Storm, D.; Aliprantis, A. O. The collection of NFATc1-dependent transcripts in the osteoclast includes numerous genes non-essential to physiologic bone resorption. *Bone* **2012**, *51*, 902−912.

(10) He, C. C.; Hui, R. R.; Tezuka, Y.; Kadota, S.; Li, J. X. Osteoprotective effect of extract from *Achyranthes bidentata* in ovariectomized rats. *J. Ethnopharmacol.* **2010**, *127*, 229−234.

(11) Li, J. X.; Hareyama, T.; Tezuka, Y.; Zhang, Y.; Miyahara, T.; Kadota, S. Five new oleanolic acid glycosides from *Achyranthes bidentata* with inhibitory activity on osteoclast formation. *Planta Med.* **2005**, *71*, 673−679.

(12) Li, J. F.; Zhao, Y.; Cai, M. M.; Li, X. F.; Li, J. X. Synthesis and evaluation of a novel series of heterocyclic oleanolic acid derivatives with anti-osteoclast formation activity. *Eur. J. Med. Chem.* **2009**, *44*, 2796−2806.

(13) Zhao, Y.; Huai, Y.; Jin, J.; Geng, M.; Li, J. X. Quinoxaline derivative of oleanolic acid inhibits osteoclastic bone resorption and prevents ovariectomy-induced bone loss. *Menopause* **2011**, *18*, 690−697.

(14) Vernall, A. J.; Hill, S. J.; Kellam, B. The evolving small-molecule fluorescent-conjugate toolbox for Class A GPCRs. *Br. J. Pharmacol.* **2014**, *171*, 1073−1084.

(15) Mizukami, S.; Hori, Y.; Kikuchi, K. Small-molecule-based protein-labeling technology in live cell studies: probe-design concepts and applications. *Acc. Chem. Res.* **2014**, *47*, 247−256.

(16) Hida, T.; Fukui, Y.; Kawata, K.; Kabaki, M.; Masui, T.; Fumoto, M.; Nogusa, H. Practical application of oxidation using a novel Na_2WO_4-H_2O_2 system under neutral conditions for scale-up manufacturing of 12α-hydroxy-3-oxooleanano-28,13-lactone: key intermediate of endothelin A receptor antagonist S-0139. *Org. Process Res. Dev.* **2010**, *14*, 289−294.